Research Article

Metabolic systems analysis identifies a novel mechanism contributing to shock in patients with endotheliopathy of trauma (EoT) involving thromboxane A2 and LTC_4

Hanne H. Henriksen [a,b], Igor Marín de Mas [b,c], Helena Herand [b,c], Joseph Krocker [d], Charles E. Wade [d] and Pär I. Johansson [a,b,d*]

***a* - Department of Clinical Immunology,** *Copenhagen University Hospital, Rigshospitalet, Copenhagen, Denmark*
***b* - CAG Center for Endotheliomics,** *Copenhagen University Hospital, Rigshospitalet, Denmark*
***c* - Novo Nordisk Foundation Center for Biosustainability,** *Technical University of Denmark*
***d* - Center for Translational Injury Research,** *Department of Surgery, University of Texas Health Science Center, Houston, TX, USA*

Correspondence to Pär I. Johansson:*Department of Clinical Immunology, Copenhagen University Hospital, Blegdamsvej 9, Rigshospitalet, Copenhagen DK2100, Denmark. *per.johansson@regionh.dk (P.I. Johansson)*
https://doi.org/10.1016/j.mbplus.2022.100115

Abstract

Purpose: Endotheliopathy of trauma (EoT), as defined by circulating levels of syndecan-1 $\geq$ 40 ng/mL, has been reported to be associated with significantly increased transfusion requirements and a doubled 30-day mortality. Increased shedding of the glycocalyx points toward the endothelial cell membrane composition as important for the clinical outcome being the rationale for this study.
Results: The plasma metabolome of 95 severely injured trauma patients was investigated by mass spectrometry, and patients with EoT vs. non-EoT were compared by partial least square-discriminant analysis, identifying succinic acid as the top metabolite to differentiate EoT and non-EoT patients (VIP score = 3). EoT and non-EoT patients' metabolic flux profile was inferred by integrating the corresponding plasma metabolome data into a genome-scale metabolic network reconstruction analysis and performing a functional study of the metabolic capabilities of each group. Model predictions showed a decrease in cholesterol metabolism secondary to impaired mevalonate synthesis in EoT compared to non-EoT patients. Intracellular task analysis indicated decreased synthesis of thromboxanA2 and leukotrienes, as well as a lower carnitine palmitoyltransferase I activity in EoT compared to non-EoT patients. Sensitivity analysis also showed a significantly high dependence of eicosanoid-associated metabolic tasks on alpha-linolenic acid as unique to EoT patients.
Conclusions: Model-driven analysis of the endothelial cells' metabolism identified potential novel targets as impaired thromboxane A2 and leukotriene synthesis in EoT patients when compared to non-EoT patients. Reduced thromboxane A2 and leukotriene availability in the microvasculature impairs vasoconstriction ability and may thus contribute to shock in EoT patients. These findings are supported by extensive scientific literature; however, further investigations are required on these findings.

Introduction

Traumatic injury has a high mortality rate, and despite the introduction of damage control blood resuscitation to combat coagulopathy, it remains a leading cause of death worldwide [1,2]. We have previously reported that endotheliopathy is linked with developing both coagulopathy and multiorgan

failure, contributing to the high mortality observed in trauma patients with sympathetic activation as a pivotal driver, as denoted by high levels of epinephrine and norepinephrine [3,4]. A vital feature of endotheliopathy in trauma is the shedding of the endothelial glycocalyx, as measured by syndecan-1, due to a shock-induced catecholamine surge [3–5]. The glycocalyx contains a large volume (1–1.7 L) of non-circulating plasma [6], and it is negatively charged, thus counteracting microvascular thrombosis and maintaining a consistent blood flow [7]. In a cohort of 410 trauma patients, we found that a cut-off level of syndecan-1 $\geq$ 40 ng/mL was associated with significantly increased transfusion requirements and a doubled 30-day mortality, confirming the pivotal role of the glycocalyx for both hemostasis and the outcome in trauma patients, a condition entitled Endotheliopathy of Trauma (EoT) [8].

Studying the endothelium in vivo is inherently difficult since it is impossible to extract biopsies of the microvascular endothelium in patients suffering from acute critical shock. To overcome this limitation, we introduced metabolic systems analysis by entering extracellular metabolome data from patient plasma samples into a biologically validated genome-scale metabolic model of the microvascular endothelial cell (EC-GEM) [9–11]. The vascular compartment encompasses more than one trillion endothelial cells that are in constant contact with the circulating blood [12]. Previously, when parameterizing EC-GEM with the plasma metabolome from trauma patients, four shock-induced endotheliopathic phenotypes were displayed, of which one cluster depended on the syndecan-1 level [13]. Based on that finding, the present study aimed to comparatively analyze the endothelial cell metabolism in EoT vs. non-EoT patients, focusing on the glycan and lipid metabolism as these are pivotal for the cell membrane phenotype, including that of the glycocalyx [14].

Results

Clinical characteristics

The clinical characteristics of the patients revealed that EoT patients were more seriously injured (higher injury severity score; ISS), received more transfusions, were more shocked and had higher 24- and 72-hour mortality rates than non-EoT patients (Table 1).

Measurement of catecholamine levels in EoT vs. non-EoT patients

EoT patients presented with higher epinephrine and norepinephrine than non-EoT patients (Table 2).

Measured metabolites

Based on prior work with critically ill trauma patients, we selected 62 metabolites to quantify (Table 3) [13,15].

In total, eight metabolites were missing from over 30% of the samples and hence were removed from further analysis as they could not be processed by the imputation algorithm [16]. For the remaining 54 metabolites, <2% of the total values were missing from the data file. Missing values were imputed using the Missforest package [17] in RStudio (version 3.6.3), which applies a random forest approach to impute values, thereby minimally altering the statistical characteristics of the metabolite.

Outlier detection

Pareto scaling for principal component (PCA) of the measured metabolites was performed to assess the influence of outliers on the conducted EC-GEMs. Four patients were considered outliers as they presented a metabolic profile outside the 95% PCA 1–2 confidence interval (one patient in the three-dimensional plot PCA 1–3) (Supplementary Table B). The four patients had different vectors, e.g., different directions on the PCA plot. The anomalous metabolic profiles for these four patients could not be clarified by the clinical presentation and were removed from further analysis. Accordingly, 95 patients were included in the following analyses.

Plasma metabolome in EoT vs. non-EoT-patients

Partial least square-discriminant analysis (PLS-DA) was conducted on the plasma metabolome from the EoT and non-EoT patients. The top metabolite of importance in the PLS-DA plot that differentiated EoT and non-EoT patients was succinic acid (VIP score = 3). The further top-10 variables of importance from the PLS-DA comprised malic acid, propionyl-L-carnitine, ornithine, lactic acid, aspartic acid, acetyl-L-carnitine, L-kynurenine, oleic acid and alpha-ketoglutarate (Fig. 1A and B). A volcano plot was generated to display significantly different metabolites, adjusted for the false discovery rate (p-value < 0.001) and with a fold change of $\geq$ 1.5. This analysis showed that succinic acid alone is essential to differentiate EoT vs. non-EoT patients, with a fold change of $\geq$ 1.5 and adjusted p-value (fold change = 1.5372, adjusted p-value < 0.001; Fig. 2).

Genome-scale metabolic network reconstruction analysis

The presented work introduces the analysis of endothelial cells' metabolism via model-driven methods using large-scale metabolic network models, the so-called genome-scale metabolic

Table 1 Patient demographics, admission vitals, transfusions and outcomes for 95 adult trauma patients (≥18 years) who met the criteria for full trauma team activation at the Red Duke Trauma Institute of the Memorial Hermann Hospital, Houston, Texas, USA.

		Non-EoT	EoT	*p*-value
		(n = 37)	(n = 58)	
Demographics				
Age	Years	46.0 [36.0, 58.0]	44.0 [32.3, 51.0]	0.262
Sex	Male [n (%)]	25 (67.6%)	45 (77.6%)	0.400
Ethnicity	Non-Hispanic[n(%)]	29 (78.4%)	40 (69.0%)	0.713
Race	Race [n(%)]	White = 17 (45.9%) African American = 9 (24.3%) Hispanic = 8 (21.6%) Asian = 1 (2.7%) Other = 2 (5.4%)	White = 20 (34.5%) African American = 16 (27.6%) Hispanic = 14 (24.1%) Asian = 1 (1.7%) Other = 7 (12.1%)	0.727
BMI	Score	28.3 [25.3, 30.9]	27.2 [24.8, 31.4]	0.698
Injury type and severity				
ISS	Score	22.0 [9.0, 25.0]	26.0 [22.5, 34.0]	**<0.001**
AIS Head	Score	0 [0, 0]	0 [0, 0]	0.842
AIS Face	Score	0 [0, 0]	0 [0, 0]	0.195
AIS Thorax	Score	0 [0, 3]	3 [0, 4]	**0.044**
AIS Abdomen	Score	0 [0, 2]	2 [0, 4]	**0.003**
AIS Extremity	Score	0 [0, 3]	0 [0, 3]	0.171
AIS External	Score	1 [0, 2]	1 [1,2]	0.155
GCS	Score	15 [3,15]	9 [3,15]	**0.014**
ED admission physiology				
SBP	mmHg	125 [114, 139]	110 [98, 133]	**0.027**
Heart rate	Bpm	96 [81, 110]	102 [85, 120]	0.185
Lab parameters				
BE	mEq/L	−2.0 [-6.0, −2.0]	−8.0 [-11.5, −4.3]	**<0.001**
Lactate	mg/dL	3.2 [2.1, 3.8]	5.3 [2.8, 9.4]	**0.001**
Glucose	mg/dL	153 [117, 180]	181 [134, 235]	**0.013**
Creatinine	mg/dL	1.08 [0.95, 1.30]	1.36 [1.01, 1.58]	**0.002**
BUN	mg/dL	14 [12, 19]	16 [13, 20]	0.185
Transfusions pre-hospital				
Transfused pre-hospital?	Yes [n (%)]	4 (10.8%)	15 (25.9%)	0.127
If yes:				
RBC	Units	1 [1, 1]	1 [0, 1]	0.469
Plasma	Units	1 [0.5, 1]	1 [0.5, 1]	0.736
Transfusions after admission				
Transfused within four hours?	Yes [n (%)]	13 (35.1%)	42 (72.4%)	**0.001**
If yes:				
RBC	Units	2 [0, 4]	4 [2, 12]	**0.038**
Plasma	Units	3 [1, 4]	4 [1, 11]	0.317
Platelets	Units	0 [0, 0]	0 [0, 6]	0.070
Transfused within 24 h?	Yes [n (%)]	21 (56.8%)	46 (79.3%)	**0.034**
If yes:				
RBC	Units	1 [0, 3]	3.5 [1, 12]	**0.013**
Plasma	Units	6 [3, 12]	4 [1, 14]	0.771
Platelets	Units	0 [0, 0]	0 [0, 6]	**0.016**
Outcome				
Mortality (<24 h)	n (%)	1 (2.7%)	11 (19.0%)	**0.044**
Mortality (<72 h)	n (%)	1 (2.7%)	12 (20.7%)	**0.029**
Mortality (<30 days)	n (%)	10 (27.0%)	25 (43.1%)	0.172

Note: BMI, body mass index; AIS, abbreviated injury score; GCS, Glasgow coma score; SBP, systolic blood pressure; BE; base excess, BUN; blood urea nitrogen, RBC; red blood cells. Medians (IQR) or n (%) are reported. *p*-values < 0.05 are shown in bold.

models (GEMs). This systems biology tool gathers all the biochemical reactions encoded by an organism's genome and represents an excellent platform to integrate multiple omics data ranging from metabolomics [18] to transcriptomics [19], among any other omics measuring the components of a living cell. As such, genome-scale metabolic reconstruction analysis enables us to infer a case-

Table 2 ELISA measurements of catecholamine and endothelium biomarkers in 95 critically ill trauma patients.

		Non-EoT (n = 37)	EoT (n = 58)	*p*-value
ELISA measurements				
Adrenaline	pg/mL	241 [89.4, 392]	458 [206, 1800]	**0.004**
Noradrenaline	pg/mL	780 [388, 1310]	1740 [724, 3590]	**<0.001**
Syndecan-1	ng/mL	25.0 [18.9, 31.2]	161 [75.6, 192]	**<0.001**

Medians (IQR) or n (%) are reported. *p*-values < 0.05 are shown in bold.

specific metabolic flux profile (i.e., EoT or non-EoT metabolism) that ultimately leads to determining the cellular functions underlying a given phenotype.

To integrate all the measured metabolites in this study, the latest reconstruction of endothelial cell metabolism [13] was upgraded. To that end, the original model's annotation was improved and new reactions were added (see Methods). This model now accounts for 3006 reactions and 2114 metabolites (iEC3006 GEM).

Plasma metabolome data from EoT and non-EoT patient groups were integrated into the GEM reconstruction analysis as follows. First, literature-based data on endothelial cell metabolism were integrated as constraints into the iEC3006 model, together with a sampling analysis, to characterize a baseline model of endothelial cells describing the spectrum of feasible nutrients' uptake/secretion rates. The uptake/secretion rates for the EoT and non-EoT models were redefined by the mean fold change from the plasma metabolomics dataset. The recalculated uptake/secretion rates were imposed as new constraints on the iEC3006 model, and a sampling analysis was performed to characterize both EoT and non-EoT GEMs (see Methods). The resulting general iEC3006 GEM, as well as EoT and non-EoT GEMs, were uploaded to the GitHub repository (https://github.com/HHEN0042/EoT).

Validation of the GEMs reconstruction

To determine the reliability of the GEMs of EoT and non-EoT reconstructions, a cross-validation analysis was performed. Here, an EoT and non-EoT unconstrained model for each exchange reaction was reconstructed, and the corresponding population of feasible flux values for each unconstrained exchange reaction was calculated by applying a sampling analysis. Next, to determine the value of EoT and non-EoT models' predictions, the solutions from the unconstrained models were compared with the initial EoT and non-EoT constrained models, and the significance was calculated by a *t*-test. The analyses showed that the models could predict 92.45% of the metabolite uptake/secretion rates with an associated *p*-value < 0.01 and with high accuracy; the R^2 scores were 0.9992 and 0.9985 for the non-EoT and EoT groups, respectively (Supplementary Table I).

Intracellular metabolism in EoT and non-EoT patients

In total, 50 central tasks of the lipid and glycan metabolism were analyzed using the iEC3006, and we explored the two models' maximum capability to metabolize a specific product/s from a defined substrate/s (Supplementary Table E) [20]. Results are included in the supplementary material (Supplementary Table F).

Beyond this, the lipid metabolism results are displayed in a heat map (Fig. 3). Remarkably, the task analysis for cholesterol metabolism revealed a decrease in the synthesis of mevalonate that represented the activity of hydroxymethylglutaryl-CoA (HMG-CoA) reductase (86% lower in EoT compared to non-EoT group), despite a similar availability of HMG-CoA for mevalonate (Fig. 4). This reaction represents the rate-limiting step of cholesterol synthesis [21].

Further to this, in the fatty acid metabolism analysis, similar synthesis rates for both trauma groups were calculated in most of the lipid-associated tasks. However, arachidonic acid synthesis was predicted to be almost 30 times higher in EoT compared to non-EoT patients (Fig. 3). Since arachidonic acid is one of the main eicosanoid precursors, a more in-depth analysis of these molecules' metabolism and the role of arachidonic acid in fatty acid beta-oxidation was conducted.

To further investigate the metabolic implication of increased arachidonate synthesis in EoT patients, 26 new tasks describing the synthesis of the different eicosanoids noted in the model from arachidonic acid, as well as one task describing the carnitine palmitoyltransferase I (CPT1) activity, were designed (Supplementary Table G). Next, the flux through these newly defined tasks was analyzed in both EoT and non-EoT patients, with the results displayed in Fig. 5A and the corresponding data included in the supplementary material (Supplementary Table H).

EoT and non-EoT patients had similar fluxes toward prostaglandin H2, PGD_2, PGE_2 and PGF_2 (Fig. 5A and B). The analysis predicted a decrease in the synthesis of thromboxane A2 in

Table 3 Metabolites measured in the plasma.

Metabolite name
L-Alanine
Glycine
L-Valine
L-Leucine
L-Isoleucine
L-Threonine
L-Proline
Asparagine
L-Serine
L-Glutamic acid
L-Methionine
L-Phenylalanine
Ornithine
L-Lysine
L-Tyrosine
L-Tryptophan
L-Aspartic acid
L-Cystine
Pyruvate
Fumaric acid
Succinic acid
Lactate
Malic acid
(±)12(13)-DiHOME*
12(S)-HETE
13-OxoODE*
14-HDoHE
15(S)-HETE*
5-Oxoproline
Acetylcarnitine
Adenosine
α-Ketoglutarate
α-Linolenic acid
Arachidonic acid
Butyrylcarnitine*
Carnitine
Decanoylcarnitine
Dihomo-ɤ-linolenic acid
Docosahexaenoic acid
Docosapentaenoic acid
Docosatetranoic acid
Dodecanoicdioic acid
Eicosapentaenoic acid
Glucose
Hypoxanthine
Isovaleryl-L-carnitine
L-Arginine*
L-Glutamine
L-Histidine
Linoleate
L-Kynurenine
Myristoyl-L-carnitine*
N,N-dimethylglycine
Octanoylcarnitine
Oleic acid
Palmitic acid
Palmitoylcarntine*
Propionylcarnitine
Prostaglandin E2*
Sphingosine 1-phopshate
Trimethylamine N-oxide
Uric acid

Note: Metabolite marked with * were not included in the further analysis as it had a high number of missing values.

the EoT compared to non-EoT patients (Fig. 5A and B). A decrease in the synthesis of 5-HPETE, and thereby the leukotrienes (LTA_4, LTB_4) and the cysteinyl leukotriene LTC_4, were also predicted in the EoT compared to non-EoT patients (Fig. 5A and B). The mitochondrial membrane transporter CPT1 was more active in the non-EoT group (234%), indicating a higher β-oxidation activity as CPT1 transports long-chain fatty acids such as arachidonate acid into the mitochondria to be metabolized as a source of energy.

Moreover, EoT patients had decreased degradation of glycan metabolism due to keratan sulfate degradation (94.4% reduction) compared to non-EoT patients (Fig. 6).

Evaluating the association between the extracellular plasma metabolome and EC intracellular metabolic tasks

The current work proposes a novel strategy integrating plasma metabolome data in genome-scale metabolic network models to unveil the metabolic mechanisms underlying the EoT phenotype. To test this strategy, we applied constraint-based modeling methods to infer the metabolic flux profiles through a set of metabolic tasks [20] in both EoT and non-EoT patients.

This approach relies on the fact that more than one trillion endothelium cells (ECs) lines the inside of the vascular compartment and are in direct contact with the circulating blood, and thereby, the plasma, in which any changes observed consequently largely reflect endothelium cell metabolism.

To test this assumption, a sensitivity analysis evaluating the impact of the measured metabolites' perturbations on metabolic tasks was performed (see Methods). Clustering analysis was then carried out on the sensitivity analysis to find groups of tasks potentially correlated with specific extracellular metabolites. The results showed a cluster of eicosanoid-associated tasks in both EoT and non-EoT models. This cluster is highly sensitive to variations in arachidonic acid and alpha-linolenic acid in the EoT model but only to arachidonic acid in the non-EoT model, indicating that alpha-linoleic acid dependence is a unique feature of the EoT group (Fig. 7).

Discussion

In the present study, we confirmed that EoT patients were more severely injured (higher ISS), more shocked (lower systolic blood pressure and base excess), had higher transfusion requirements and had higher early mortality rates (mortality before one day and also before three days) compared to non-EoT patients (Table 1) [9,16]. Shedding of the endothelial glycocalyx releases significant constituents into the circulating

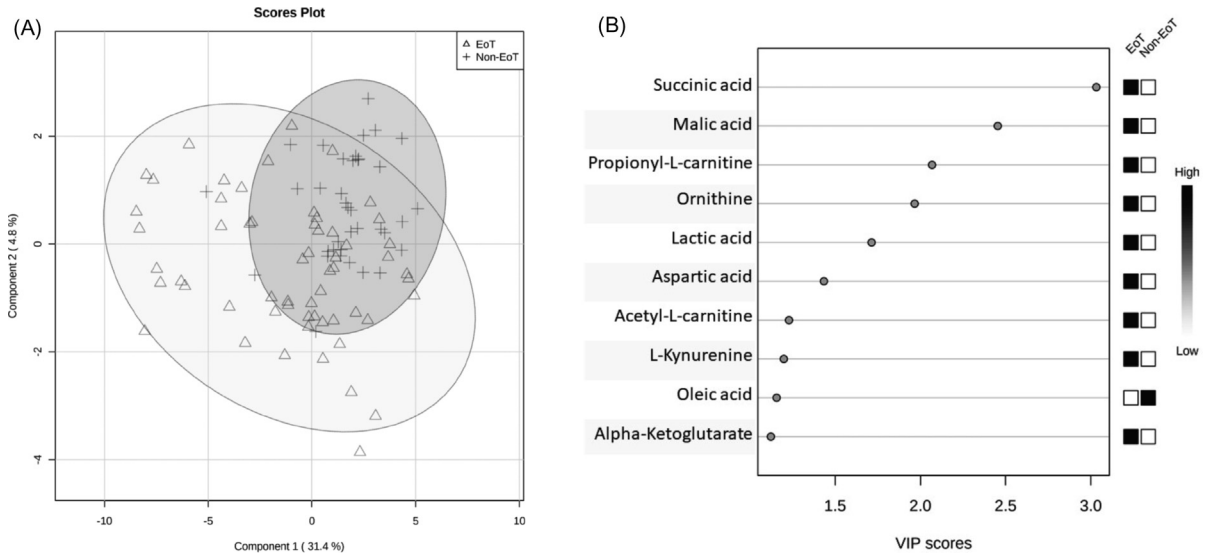

Fig. 1. PLS-DA identifies different metabolic profiles for EoT and non-EoT patients.A. PLS-DA score plot to differentiate EoT and non-EoT patients. B. VIP score plot illustrating the top-10 important variables in the PLS-DA analysis.

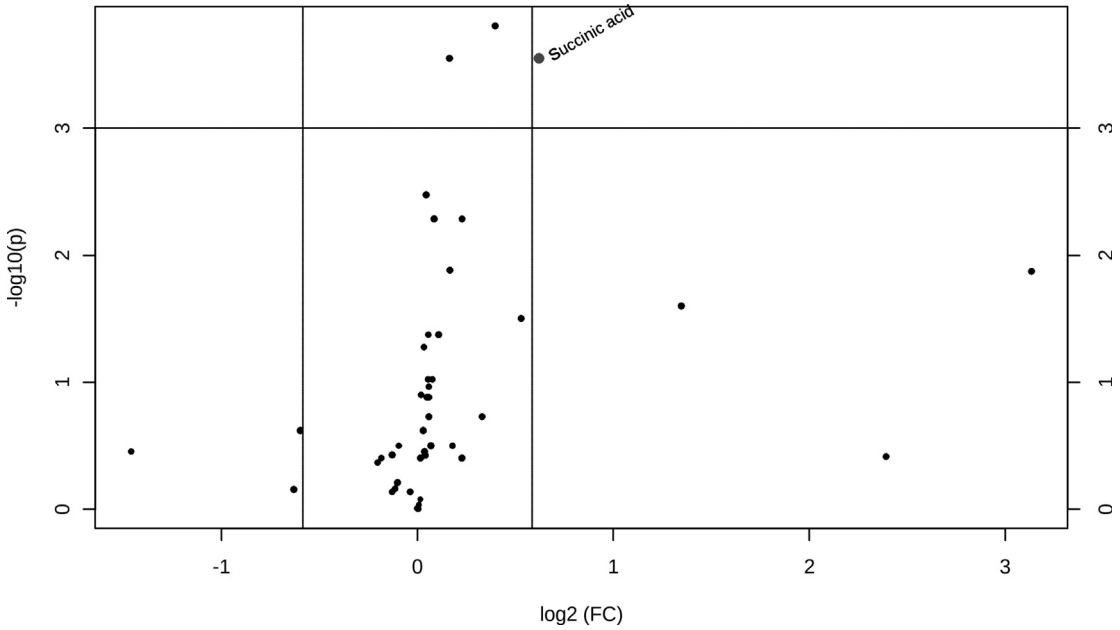

Fig. 2. Volcano plot identifying succinic acid as essential to differentiate between EoT and non-EoT patients.Note: The volcano plot has an adjusted false discovery rate (p-value < 0.001) and a fold change $\geq$ 1.5.

blood, rendering it hypercoagulable, and this likely contributes to the increased transfusion requirements observed in EoT patients [22].

PLS-DA, in combination with a volcano plot representation, were performed to identify significantly important plasma metabolites, to differentiate between EoT and non-EoT patients. Both analyses highlighted succinic acid as the top metabolite of importance in differentiating between EoT and non-EoT patients, with increased levels in EoT patients. Increased succinic acid levels observed in EoT patients aligned with our previous findings in a pilot trauma study, which showed one phenotype dependent on syndecan-1 levels, with increased succinic acid levels compared to the other phenotypes [9]. Furthermore, D´Alessandro and colleagues reported that in a cohort of 95 severely injured trauma patients, succi-

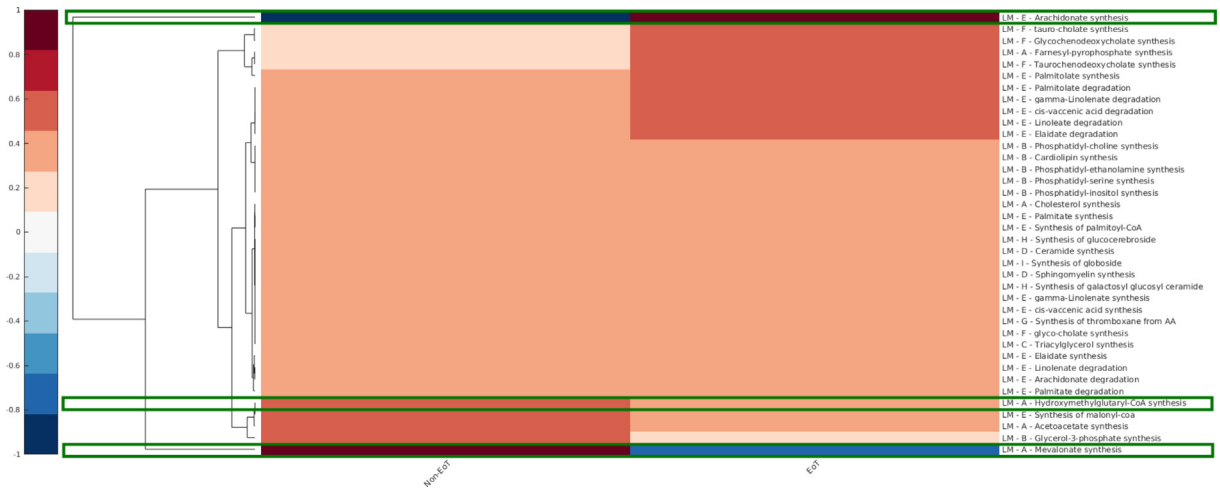

Fig. 3. Heat map of the predicted metabolic flux throughout the tasks corresponding to lipid metabolism in EoT and non-EoT EC-GEMs.Note: All the fluxes are scaled between −1 and 1. Relevant tasks are marked in green boxes. LM: lipid metabolism, A: cholesterol metabolism, B: glycerophospholipid metabolism, C: triacylglycerol metabolism, D: sphingolipid metabolism, E: fatty acid metabolism, F: bile acid synthesis, G: eicosanoid metabolism, H: ganglioside metabolism, I: globoside metabolism, J: GPI anchor biosynthesis, K: N-glycan metabolism, L: O-glycan metabolism, M: keratan sulfate metabolism. (For interpretation of the references to colour in this figure legend, the reader is referred to the web version of this article.)

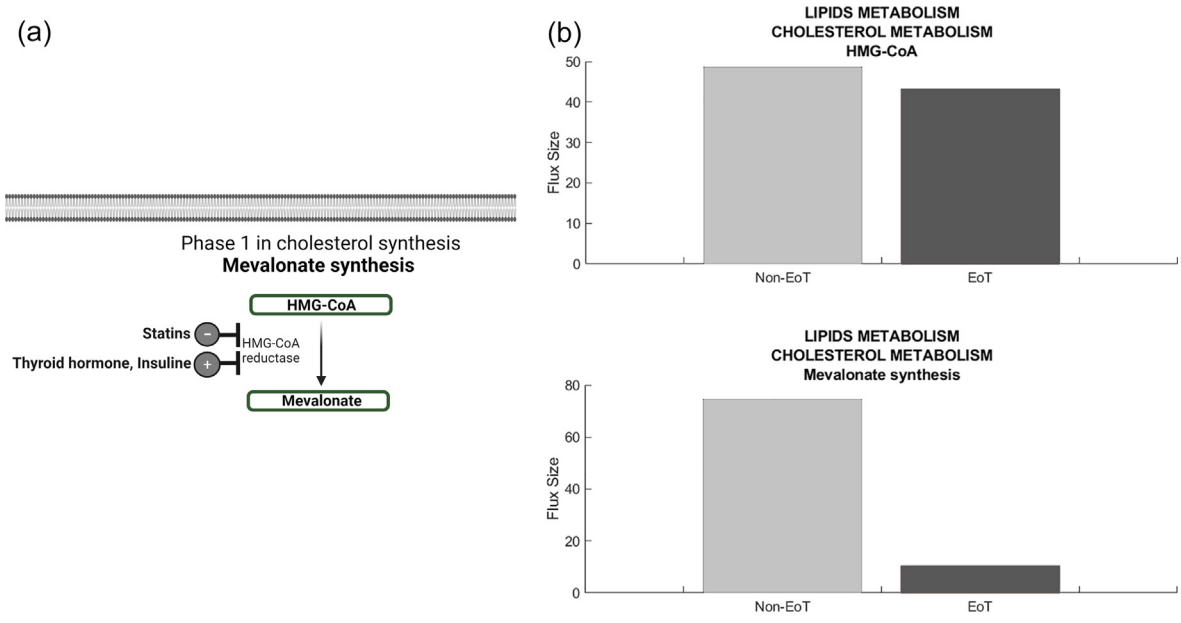

Fig. 4. EoT patients appear to present with decreased cholesterol metabolism caused by impaired mevalonate synthesis.A. Synthesis of mevalonate from HMG-CoA via HMG-CoA reductase. Mevalonate is synthesized from HMG-CoA and stimulated by the enzyme HMG-CoA-reductase. Statins inhibit the enzyme HMG-CoA-reductase and thereby decrease mevalonate synthesis. Thyroid hormones and insulin have an agonistic effect by stimulating the HMG-CoA reductase enzyme's activity. B. Predicted HMG-CoA synthesis and mevalonate synthesis flux from HMG-CoA in non-EoT and EoT EC-GEMs. The flux size is given in mmol per gDW per hr.

nate levels were significantly higher in patients who died compared to survivors [23]. Similarly, elevated levels of succinic acid have been observed in animal studies undergoing shock [24,25]. In addition, the glutamine pathways, an alternative substrate for ATP production in anaerobic settings, have been

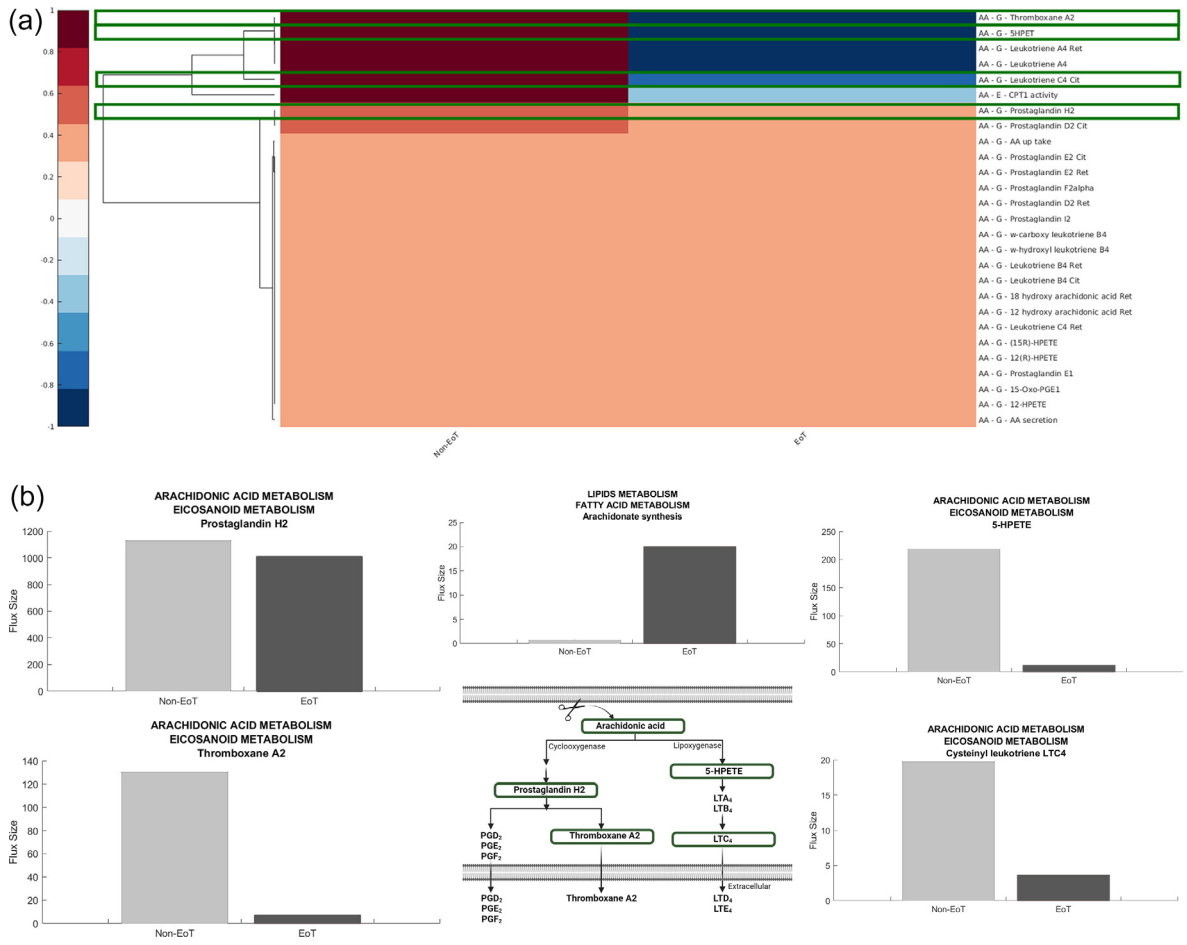

Fig. 5. EoT patients appear to present decreased arachidonate synthesis and secondary decreased production of eicosanoids (thromboxane A2, leukotrienes and cysteinyl leukotriene LTC_4).A. Heat map of the predicted metabolic flux throughout all tasks corresponding to arachidonate acid metabolism in EoT and non-EoT EC-GEMs. All fluxes are scaled between −1 and 1. Relevant tasks are marked in green boxes. AA: arachidonate acid, E: fatty acid metabolism, G: eicosanoid acid metabolism. B. Eicosanoid metabolism, describing the metabolization of arachidonate into different eicosanoid species. Predicted arachidonate, prostaglandin H2, thromboxane A2, 5-HPETE and cysteinyl leukotriene LTC4 synthesis flux in non-EoT and EoT EC-GEMs. The flux size is given in mmol per gDW per hr. (For interpretation of the references to colour in this figure legend, the reader is referred to the web version of this article.)

shown to result in an increased level of succinic acid under shock [26].

Succinic acid plays a crucial role in ATP formation in the mitochondria. However, mitochondrial membrane dysfunctionality leads to succinic acid accumulation [27]. Increased succinic acid levels have also been linked with an increase in inflammation, resulting in organ failure [28]. Therefore, one may hypothesize that the elevated levels of succinic acid in the EoT populace is forced by a mitochondrial dysfunction, which results in a second hit after the initial trauma hit.

To investigate the intracellular response in endothelial cells of EoT vs. non-EoT patients, we generated two GEMs using the iEC3006 model and performed a task analysis focused on glycan and lipid metabolism. Interestingly, the intracellular metabolic fluxes showed a significant decrease in the activity of HMG-CoA reductase (mevalonate synthesis task), a rate-limiting reaction in cholesterol metabolism, in EoT patients compared to non-EoT patients. The cell membrane consists of 25–30% cholesterol, the highest concentration of lipids in the membrane [29]. Hence, cholesterol plays a vital role in the membrane function, where it regulates membrane fluidity by reducing the permeability of the cell membrane, which it achieves by increasing the packing of phospholipids, thereby helping to restrict the passage of molecules [29]. The significant reduction in mevalonate synthesis and consequently cholesterol observed in the EoT patients may, therefore, increase the membrane flu-

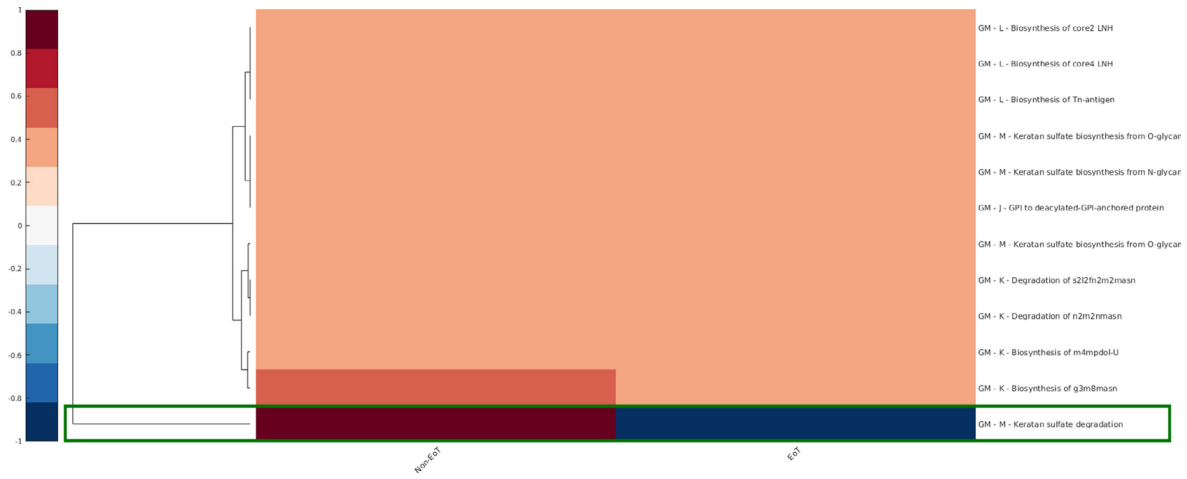

Fig. 6. EoT patients appear to present decreased keratan sulfate metabolism.Heat map of the predicted metabolic flux throughout all tasks corresponding to glycan metabolism in EoT and non-EoT EC-GEMs. All fluxes are scaled between −1 and 1. Relevant task is marked in a green box. GM: glycan metabolism, J: GPI anchor biosynthesis, K: N-glycan metabolism, L: O-glycan metabolism, M: keratan sulfate metabolism. (For interpretation of the references to colour in this figure legend, the reader is referred to the web version of this article.)

idity and permeability, besides the direct toxic effects of catecholamines generated by the trauma [29,30]. Furthermore, mevalonate production is pivotal for the antioxidants' defense system as it produces coenzyme Q10, which is crucial for the electron transport of the mitochondrial respiratory chain [31]. The significant decrease in mevalonate in EoT patients observed here may thus result in abnormal mitochondrial respiratory function and increase the levels of free radicals. This may result in increased membrane damage by initiating lipid peroxidation of unsaturated fatty acid in the cell membranes, including in the mitochondrial membrane – thereby further disturbing the membrane integrity [32]. This highlights the importance of the sustainable production of mevalonate for cellular homeostasis and may explain the high observed extracellular levels of succinic acid, an intermediate of the respiratory cycle, in EoT patients [33]. The production of mevalonate is a rate-limiting step in cholesterol production regulated by the HMG-CoA reductase enzyme, which is the molecular target for cholesterol-lowering statins [34,35]. Interestingly, statins have been associated with decreased mortality in numerous cancer types, linked to the primary tumor suppressor gene p53, whereby downregulation of the mevalonate pathway occurs when stress mediators activate p53 [36]. Therefore, one could speculate that p53 is implicated in the decrease in mevalonate observed in EoT patients due to "overactivation" of p53 caused by severe stress mediators.

Furthermore, an increase in arachidonate synthesis was also observed in patients with EoT. Arachidonate, an esterified arachidonic acid (AA), is naturally found incorporated in the structural phospholipids in the cell membranes throughout the body [37]. AA is released from the membrane phospholipids by phospholipase A2, phospholipase and phospholipase D. Free AA will then be metabolized into the eicosanoids, e.g., small signal-molecules, which through the cyclooxygenase and lipoxygenase pathways can either be transformed into prostaglandins, thromboxanes or leukotrienes [38]. The release of AA from the cell membrane is forced by high levels of circulating stress mediators such as the shock-induced catecholamine surge and accompanying inflammation [39]. In case of inflammation or shock, eicosanoids will act as pro-inflammatory molecules (prostaglandin H2), platelet aggregating factors (thromboxane A2), modifiers of vascular permeability (leukotrienes) and vasoconstrictors (thromboxane A2, cysteinyl leukotrienes) [40–42]. To further investigate the fate of arachidonic acid metabolization, we analyzed pathways only focusing on the eicosanoids, and interestingly, we observed that thromboxane A2, leukotrienes and cysteinyl leukotriene LTC_4 were decreased in EoT compared to non-EoT patients. A pivotal function of both thromboxane A2 and LTC_4 is vasoconstriction [43], and loss of this results in refractory circulatory shock. That was corroborated by EoT patients in the present study, who presented with lower blood pressure, along with higher base excess and lactate levels, compared to non-EoT patients. A further pivotal function of thromboxane A2 is to stimulate the activation of new platelets, as well as increase platelet aggregation and thus support hemostasis [44]. It could be speculated that the reduction of thromboxane A2 in EoT patients impairs hemostatic competence, also contributing to the increased transfusion

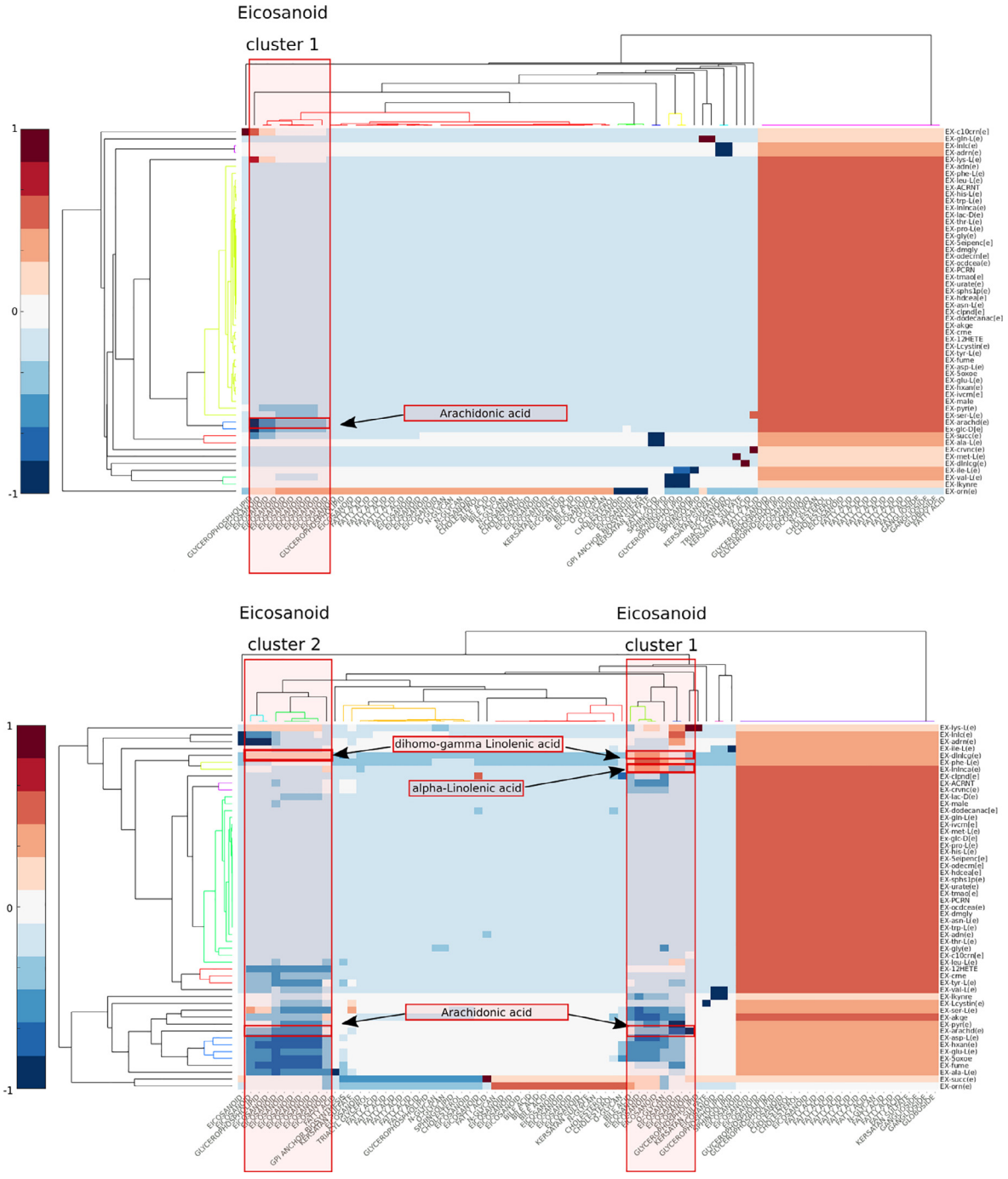

Fig. 7. Sensitivity analysis associating extracellular metabolites and intracellular metabolic tasks.Note: A. Sensitivity analysis of the non-EoT EC-GEM. B. Sensitivity analysis of the EoT EC-GEM.

requirements observed, and thus warrants further investigation.

Additionally, the role of AA as a regulator of cholesterol metabolism has been reported; this could imply the peroxidation of AA associated with different pathologies [45] may explain the predicted lower utilization of AA as a source of eicosanoid or β-oxidation metabolism. These findings suggest a common mechanism underlying the differences observed between EoT and non-EoT patients [46], which requires further investigation.

Beyond this, non-EoT patients displayed increased degradation of keratan sulfate, a constituent of the endothelial glycocalyx [47]. Keratan sulfate glycosaminoglycans' expression in the vasculature, and its importance in (patho)physiology, are less well-understood, requiring further investigation [47,48].

In addition, a sensitivity analysis was performed to investigate the interdependence between the plasma exometabolome and the intracellular task activity, showing an eicosanoid-associated task cluster highly sensitive to changes in alpha-linolenic acid only in the EoT group. Interestingly, these findings are in accordance with abundant literature associating alpha-linolenic acid with inflammation and alterations to the cell membrane and its permeability [49–51] that are characteristic of the EC phenotype in EoT patients. Thus, this analysis shows that relevant correlations between the plasma sample metabolites and metabolic task predictions are consistent with experimental observations connecting endothelial cell metabolism and phenotypes, which supports the integration of plasma metabolome data into GEM reconstruction analyses as a novel approach to studying ECs' metabolism.

The present study has limitations inherent to observational studies, and the results are consequently mere associations. Furthermore, a limited number of trauma patients were included and from one center only. Moreover, we hypothesize that plasma changes are primarily attributable to the EC since 1 trillion EC are in contact with the circulating blood. Yet, we cannot exclude the influence of metabolites from sources, such as muscles, lipocytes, and the liver, etc. Although the endothelial cell GEM applied here is the most detailed to date, only limited coverage of metabolic reactions is detailed. Moreover, this study focused on endothelial glycan and lipid metabolism only. Therefore, the results from the EC-GEM must be emphasized as hypothesis-generating results that require additional investigation.

In conclusion, metabolomic systems analysis of trauma patients indicates that EoT, defined by a circulating syndecan-1 level $\geq$ 40 ng/mL, is associated with alterations to the central metabolic pathways of the endothelial cell membrane, including cholesterol, fatty acid and keratan sulfate metabolism. The reduced production of eicosanoids (thromboxane A2, leukotrienes and cysteinyl leukotriene) in EoT patients appears to provide a novel potential pathophysiological mechanism that may contribute to increased shock and high mortality secondary to impaired vasoconstriction. Considering the clinical relevance of this pathology and the technical difficulties in studying endothelial cells compared to other cell types involved in human diseases, the computational methodology applied in this work provides, to our best knowledge, a unique tool for in vivo studies of the metabolic dysregulations associated with endotheliopathy. The data collectively support the proposal that metabolic systems analysis of endothelial cells may identify novel potential therapeutic opportunities for severely injured trauma patients, which warrant further investigation.

Materials and methods

Setting and patients

All critically ill adult trauma patients ($\geq$18 years) admitted directly from the injury scene to the highest level of activation at the Red Duke Trauma Institute between March 2013 and February 2018, at Memorial Hermann Hospital, Houston, Texas, USA, were included in a biorepository observational cohort study. This study was approved by the McGovern Medical School at UTHealth's institutional review board (HSC-GEN-12-0059) and is in line with the Declaration of Helsinki. Blood samples were collected immediately on the patient's arrival by on-call research assistants. Informed consent was obtained from the patient, or if the patient was unconscious, from a legally authorized representative within 72 h after enrollment. A waiver of consent was granted if the patient was discharged or died within 24 h, or three or more attempts were made to obtain consent within 72 h. If the consent could not be obtained, the patient was excluded from the study and their blood samples were destroyed.

Patient selection

Patients in this study were randomly selected retrospectively for enrollment based on the ISS from a biorepository of over 6500 patients requiring the highest level of trauma activation. In total, 20 trauma patients with minor and moderate trauma injury (ISS <16), 40 with serious trauma injury (ISS 16–25) and 39 with severe trauma (ISS >25) were included. The criterion for exclusion was a severe non-survivable traumatic brain injury. Clinical data in the registry were recorded on the patient's admission by research assistants or extracted from medical records and the trauma registry.

Definition of EoT: The clinical diagnosis of EoT in the selected cohort of trauma patients was based on an admission level of syndecan-1 $\geq$ 40 ng/mL [8].

Healthy volunteers

We previously examined 20 healthy volunteers to calculate normal metabolic variances, to incorporate metabolic patient data into the EC-GEM [13].

Analysis of clinical characteristics

Statistical analysis was performed using RStudio (version 3.6.3). Descriptive data are presented as medians with interquartile ranges (IQRs) or as a percentage (%). Non-parametric statistical tests (Mann–Whitney U test and chi-squared/Fisher's exact test) were used to evaluate unpaired group differences as appropriate.

Sample preparation

Blood samples were obtained on the patient's hospital admission in 3.2% citrated tubes. The tubes were immediately centrifugated at 1800 g for 10 min at 5 °C, completed two times in total, to separate the plasma, which was aliquoted and frozen at −80 °C for later analysis.

Enzyme-linked immunosorbent assay (ELISA) measurement

The soluble biomarkers of sympathoadrenal activation (epinephrine and norepinephrine) and endothelial glycocalyx (syndecan-1) were measured through an enzyme-linked immunosorbent assay according to the manufacturer's recommendations.

The following manufacturers were used: epinephrine and norepinephrine 2-CAT ELISA, Labor Diagnostica Nord GmbH Co. & KG, Nordhorn, Germany) and syndecan-1 (Diaclone Nordic Biosite, Copenhagen, Denmark).

Mass spectrometry analysis

Ultra-high performance liquid chromatography-mass spectrometry analysis was performed as previously published [52]. This was run on a Vanquish UHPLC system (Thermo Fisher Scientific, San Jose, CA, USA) with a Q Exactive mass spectrometer (HF Hybrid Quadrupole-Orbitrap, Thermo Fisher Scientific, San Jose, CA, USA). An electrospray ionization interface was used as an ionization source. The analysis was performed in negative and positive ionization modes. A QC sample was analyzed in MS/MS mode to identify compounds. The UPLC was performed using the protocol described by Catalin et al. with a slightly modified version where the derivatization reaction was stopped by the addition of chloroform [53]. Peak areas were extracted using a Compound Discoverer 2.0 (Thermo Scientific).

Gas chromatography-mass spectrometry was used to detect amino and non-amino organic acids. The analysis was performed using gas chromatography (7890B, Agilent) coupled with a quadrupole mass spectrometry detector (5977B, Agilent). The system was controlled by Chemstation (Agilent). Raw data were converted to a netCDF format using Chemstation (Agilent), before the data were imported and processed in MATLAB R2018b (Mathworks, Inc.) using the PARADISe software described by Johnsen et al. [54]. The mass spectrometry analyses were carried out by MS-Omics (https://www.msomics.com/).

Analysis of mass spectrometry data

Two-way comparisons were performed between patients (EoT vs. non-EoT) using the metabolomics package in RStudio (version 3.6.3). The quantified metabolic data were normalized by log2 transformation and Pareto scaling for PCA, PLS-DA and volcano plot analyses. Fumaric acid was removed from the metabolic statistical analysis as it correlated 1:1 with malic acid.

Endothelial genome-scale metabolic model upgrading

To investigate the metabolic differences between EoT and non-EoT groups, the latest reconstruction of the human endothelial cell metabolism (iEC2997 GEM) [13] was updated and expanded to enable more efficient integration of metabolic datasets (iEC3006 GEM).

Exometabolomic data (i.e., blood samples) are typically incorporated in GEM-based analyses as constraints on the exchange reactions. These reactions describe the boundaries of the model, providing information about the metabolic capabilities of the cell, which enables the quantification of the nutrients' uptake/secretion rates. Thus, the integration capacity, and consequently the predictive capabilities of the iEC3006 GEM, can be enhanced by improving the annotation and increasing the number of extracellular metabolites in the model, together with their associated exchange and transport reactions. The model upgrade was achieved in three steps: i. To improve the annotation of the measured metabolites in iEC3006 GEM, the external-database IDs of the metabolites in the model were curated to correct mis-annotations, and new IDs were added; ii. For those extracellular metabolites annotated in the model without an associated exchange reaction, new exchange and transport reactions were exported from other already-built models (i.e., Recon 2.2 or Recon 3D); iii. For those metabolites not annotated as an extracellular metabolite in the model, the extracellular annotation was included together with the associated exchange reaction and the corresponding transport reaction that was supported by the literature. As a result, the upgraded model (hereinafter iEC3006) could perform a full metabolomics dataset integration. The process is described in detail in Supplementary Table C.

Construction of EoT and non-EoT genome-scale metabolic endothelial models

To infer the metabolic flux profile of EoT and non-EoT groups that ultimately determines the cellular functions underlying a given phenotype, quantified metabolic data were integrated into the upgraded iEC3006 model using the Cobra toolbox in MATLAB R2017b [55,56]. First, a baseline model was determined by random sampling flux analysis of the constrained iEC3006 model. Next, the maximum and minimum uptake/secretion rates of all the metabolites in the baseline model were determined by the upper and lower quartiles of their respective exchange reaction flux distributions, as

determined by random sampling flux analysis of the constrained iEC3006 model.

Finally, the EoT and non-EoT models were ready to be reconstructed. To this end, the minimum and maximum uptake/secretion rates of the exchange reaction for all the measured metabolites were redefined as a function of the mean fold change (patient phenotype/20 healthy volunteers) from the plasma metabolomics dataset (more detail in Supplementary Table A). Finally, the metabolic flux profile of each model was calculated by applying random sampling flux analysis while imposing the previously defined thresholds; if necessary, reactions were relaxed to obtain a feasible model (Supplementary Table D). As a result, EoT and non-EoT genome-scale metabolic endothelial models were constructed. Finally, the reliability of model reconstruction was evaluated by comparing the exometabolomic experimental data and the model predictions via cross-validation analysis [57].

Analyzing metabolic capabilities of EoT and non-EoT genome-scale metabolic endothelial models

A functional metabolic path can be defined as the set of reactions that a living cell must activate to synthesize a given metabolite(s) from one or several substrates. These functional metabolic paths can describe specific cellular tasks necessary for cell viability in a specific condition (s). In this work, we combined a set of manually curated metabolic tasks described by Richelle et al. with flux balance analysis (FBA) to investigate the cellular capabilities of EoT and non-EoT patients [20,58]. FBA, which is implemented in the MATLAB COBRA toolbox, permits the maximum flux that a metabolic network can carry between two models of metabolites under a given set of constraints to be calculated [52]. In total, 50 central tasks in lipid and glycan metabolism were investigated (Supplementary Table E) [20].

Eicosanoid metabolization

To follow the flux from arachidonate acid to different eicosanoids, 27 paths of interest associated with eicosanoid metabolism were analyzed (Supplementary Table G).

Sensitivity analysis to evaluate the association between exometabolome and metabolic tasks

To evaluate how sensitive the different metabolic tasks defined in this work are to alterations in the metabolites' availability, a combination of sensitivity and clustering analysis was performed.

In this process the effects of perturbing individual extracellular metabolite uptake/secretion rates on each metabolic task were calculated. Here, for each measured metabolite, the flux spectrum of the associated exchange reaction, defined by the upper and lower flux values previously calculated, was divided by the number of iterations (100 in this study) in regular segments. In other words, if the upper and lower boundaries of a given exchange reaction are 1 and 100, respectively, and are divided into 100 regular segments, the value of each segment will be 1, 2, 3, ... until reaching 100. Next, the flux of each task was calculated while fixing the uptake/secretion rate of the specific metabolite to the value of each segment. As a result of this, a cubic matrix with dimensions corresponding to the number of plasma metabolites, number of tasks and number of iterations was generated for each model. In this specific case, a cubic matrix of dimensions $53\times83\times100$ (metabolites $\times$ tasks $\times$ iterations) for each EoT and non-EoT model was generated. Next, the gradient slope was calculated for each metabolite in each task, and the results were normalized and scaled to values between -1 and 1. Finally, a clustering analysis was applied to the sensitivity analysis results, and a heat-map—in combination with a dendrogram—was generated using the clustergram package in MATLAB [59].

DECLARATION OF COMPETING INTEREST

The authors declare that they have no known competing financial interests or personal relationships that could have appeared to influence the work reported in this paper.

Acknowledgments

Figures have been created with BioRender.com. HHH would like to thank the Candys Foundation for their provision of a grant (no. 2018-279). IMM would like to thank the Novo Nordisk Foundation for its two grants provided (nos. NNF10CC1016517 and NNF14OC0009473).

Funding

HHH has been supported by a PhD scholarship from Rigshospitalet, Denmark.

Appendix A. Supplementary data

Supplementary data to this article can be found online at https://doi.org/10.1016/j.mbplus.2022.100115.

Received 7 October 2021;
Accepted 14 June 2022;
Available online 18 June 2022

Keywords:
Trauma;
Metabolomics;
Endotheliopathy;
Systems biology;
Genome-scale metabolic model;
Eicosanoid

Abbreviations:
AA, Arachidonic acid; CPT1, Carnitine palmitoyltransferase I; EC, Endothelial cell; EC-GEM, Genome-scale metabolic model of the microvascular endothelial cell; EoT, Endotheliopathy of trauma; ELISA, Enzyme-linked immunosorbent assay; FBA, Flux balance analysis; GEMs, Genome-scale metabolic models; HMG-CoA, Hydroxymethylglutaryl-CoA; ISS, Injury Severity Score; LTC_4, Leukotriene C4; PCA, Principal Component Analysis; PLS-DA, Partial least square-discriminant analysis

References

[1]. Cotton, B.A., Reddy, N., Hatch, Q.M., LeFebvre, E., Wade, C.E., Kozar, R.A., Gill, B.S., Albarado, R., McNutt, M.K., Holcomb, J.B., (2011). Damage control resuscitation is associated with a reduction in resuscitation volumes and improvement in survival in 390 damage control laparotomy patients. *Ann Surg.*, **254** (4), 598–605.

[2]. Mathers, CD,. Loncar D,. (2006). Projections of global mortality and burden of disease from 2002 to 2030. PLoS Med. 3 (11), e442.

[3]. Johansson, P.I., Stensballe, J., Rasmussen, L.S., Ostrowski, S.R., (2011). A high admission syndecan-1 level, a marker of endothelial glycocalyx degradation, is associated with inflammation, protein C depletion, fibrinolysis, and increased mortality in trauma patients. *Ann Surg.*, **254** (2), 194–200.

[4]. Johansson, P.I., Stensballe, J., Rasmussen, L.S., Ostrowski, S.R., (2012). High circulating adrenaline levels at admission predict increased mortality after trauma. *J Trauma Acute Care Surg.*, **72** (2), 428–436.

[5]. Johansson, P.I., Henriksen, H.H., Stensballe, J., Gybel-Brask, M., Cardenas, J.C., Baer, L.A., Cotton, B.A., Holcomb, J.B., Wade, C.E., Ostrowski, S.R., (2017). Traumatic Endotheliopathy: A Prospective Observational Study of 424 Severely Injured Patients. *Ann Surg.*, **265** (3), 597–603.

[6]. Rehm, M., Zahler, S., Lötsch, M., Welsch, U., Conzen, P., Jacob, M., Becker, B.F., (2004). Endothelial glycocalyx as an additional barrier determining extravasation of 6% hydroxyethyl starch or 5% albumin solutions in the coronary vascular bed. *Anesthesiology.*, **100** (5), 1211–1223.

[7]. Alphonsus, C.S., Rodseth, R.N., (2014). The endothelial glycocalyx: a review of the vascular barrier. *Anaesthesia.*, **69** (7), 777–784.

[8]. Gonzalez Rodriguez, E., Ostrowski, S.R., Cardenas, J.C., Baer, L.A., Tomasek, J.S., Henriksen, H.H., Stensballe, J., Cotton, B.A., Holcomb, J.B., Johansson, P.I., Wade, C. E., (2017). Syndecan-1: A Quantitative Marker for the Endotheliopathy of Trauma. *J Am Coll Surg.*, **225** (3), 419–427.

[9]. Mo, M.L., Palsson, B.Ø., Herrgård, M.J., (2009). Connecting extracellular metabolomic measurements to intracellular flux states in yeast. *BMC Syst Biol*, **3**, 37.

[10]. Cakir, T., Efe, C., Dikicioglu, D., Hortaçsu, A., Kirdar, B., Oliver, S.G., (2007). Flux balance analysis of a genome-scale yeast model constrained by exometabolomic data allows metabolic system identification of genetically different strains. *Biotechnol Prog.*, **23** (2), 320–326.

[11]. Aurich, M.K., Paglia, G., Rolfsson, Ó., Hrafnsdóttir, S., Magnúsdóttir, M., Stefaniak, M.M., Palsson, B.Ø., Fleming, R.M., Thiele, I., (2015). Prediction of intracellular metabolic states from extracellular metabolomic data. *Metabolomics.*, **11** (3), 603–619.

[12]. Galley, H.F., Webster, N.R., (2004). Physiology of the endothelium. *British Journal of Anaesthesia.*, **93** (1), 105–113.

[13]. Henriksen, H.H., McGarrity, S., Sigurãardóttir, R.S., Nemkov, T., D'Alessandro, A., Palsson, B.O., Stensballe, J., Wade, C.E., Rolfsson, O., Johansson, P. I., (2020). Metabolic Systems Analysis of Shock-Induced Endotheliopathy (SHINE) in Trauma: A New Research Paradigm. *Ann Surg.*, **272** (6), 1140–1148.

[14]. Pries, A.R., Secomb, T.W., Gaehtgens, P., (Sep 2000). The endothelial surface layer. *Pflugers Arch.*, **440** (5), 653–666.

[15]. D'Alessandro, A., Moore, H.B., Moore, E.E., Wither, M., Nemkov, T., Gonzalez, E., Slaughter, A., Fragoso, M., Hansen, K.C., Sillimann, C.C., Banerjee, A., (2015). Early hemorrhage triggers metabolic responses that build up during prolonged shock. *Am J Physiol Regul Integr Comp Physiol.*, **308** (12), R1034. R1044.

[16]. Kokla, M., Virtanen, J., Kolehmainen, M., Paananen, J., Hanhineva, K., (2019). Random forest-based imputation outperforms other methods for imputing LC-MS metabolomics data: a comparative study. *BMC Bioinformatics.*, **20** (1), 492.

[17]. Stekhoven, D.J., Bühlmann, P., (2012). MissForest–nonparametric missing value imputation for mixed-type data. *Bioinformatics.*, **28** (1), 112–118.

[18]. Volkova, S., Matos, M.R.A., Mattanovich, M., Marín de Mas, I., (2020). Metabolic Modelling as a Framework for Metabolomics Data Integration and Analysis. *Metabolites.*, **10** (8), 303.

[19]. Marín de Mas, I., Torrents, L., Bedia, C., Nielsen, L.K., Cascante, M., Tauler, R., (2019). Stoichiometric gene-to-reaction associations enhance model-driven analysis performance: Metabolic response to chronic exposure to Aldrin in prostate cancer. *BMC Genomics*, **20** (1)

[20]. Richelle, A,. Kellman, BP,. Wenzel, AT,. Chiang, AWT,. Reagan, T,. Gutierrez, JM,. Joshi, C,. Li, S,. Liu, JK,. Masson, H,. Lee, J,. Herirendt, L,. Trefois, C,. JuarezEF,. Bath, T,. Borland, D,. Mesirov, JP,. Robasky, K,. Lewis, NE,. (2020). What does your cell really do? Model-based assessment of mammalian cells metabolic functionalities using omics data. bioRxiv. 2020.04.26.057943.

[21]. Cortese, F., Gesualdo, M., Cortese, A., Carbonara, S., Devito, F., Zito, A., Ricci, G., Scicchitano, P., Ciccone, M. M., (2016 May). Rosuvastatin: Beyond the cholesterol-lowering effect. *Pharmacol Res.*, **107**, 1–18. https://doi.org/10.1016/j.phrs.2016.02.012. Epub 2016 Mar 2 PMID: 26930419.

[22]. Ostrowski, S.R., Johansson, P.I., (2012). Endothelial glycocalyx degradation induces endogenous heparinization in patients with severe injury and early traumatic coagulopathy. *J Trauma Acute Care Surg.*, **73** (1), 60–66.

[23]. D'Alessandro, A., Moore, H.B., Moore, E.E., Reisz, J.A., Wither, M.J., Ghasasbyan, A., Chandler, J., Silliman, C. C., Hansen, K.C., Banerjee, A., (2017). Plasma succinate is a predictor of mortality in critically injured patients. *J Trauma Acute Care Surg.*, **83** (3), 491–495.

[24]. D'Alessandro, A,. Moore, HB,. Moore, EE,. Wither, MJ,. Nemkov, T,. Gonzalez, E,. Slaughter, A,. Fragoso, M,. Hansen, KC,. Silliman, CC,. et al. (2015) Early hemorrhage triggers metabolic responses that build up during prolonged shock. American journal of physiology Regulatory, integrative and comparative physiology. ajpregu 00030 2015.

[25]. D'Alessandro, A., Slaughter, A.L., Peltz, E.D., Moore, E. E., Silliman, C.C., Wither, M., Nemkov, T., Bacon, A.W., Fragoso, M., Banerjee, A., et al., (2015). Trauma/ hemorrhagic shock instigates aberrant metabolic flux through glycolytic pathways, as revealed by preliminary (13)C-glucose labeling metabolomics. *Journal of translational medicine.*, **13**, 253. PMID: 26242576.

[26]. Slaughter, A.L., D'Alessandro, A., Moore, E.E., Banerjee, A., Silliman, C.C., Hansen, K.C., Reisz, J.A., Fragoso, M., Wither, M.J., Bacon, A.W., Moore, H.B., Peltz, E.D., (2016). Glutamine metabolism drives succinate accumulation in plasma and the lung during hemorrhagic shock. *J Trauma Acute Care Surg.*, **81** (6), 1012–1019.

[27]. Tannahill, G.M., Curtis, A.M., Adamik, J., Palsson-McDermott, E.M., McGettrick, A.F., Goel, G., Frezza, C., Bernard, N.J., Kelly, B., Foley, N.H., Zheng, L., Gardet, A., Tong, Z., Jany, S.S., Corr, S.C., Haneklaus, M., Caffrey, B.E., Pierce, K., Walmsley, S., Beasley, F.C., Cummins, E., Nizet, V., Whyte, M., Taylor, C.T., Lin, H., Masters, S.L., Gottlieb, E., Kelly, V.P., Clish, C., Auron, P. E., Xavier, R.J., O'Neill, L.A.J., (2013). Succinate is an inflammatory signal that induces IL-1β through HIF-1α. *Nature.*, **496** (7444), 238–242.

[28]. Nunns, G.R., Vigneshwar, N., Kelher, M.R., Stettler, G.R., Gera, L., Reisz, J.A., D'Alessandro, A., Ryon, J., Hansen, K.C., Gamboni, F., Moore, E.E., Peltz, E.D., Cohen, M.J., Jones, K.L., Sauaia, A., Liang, X., Banerjee, A., Ghasabyan, A., Chandler, J.G., Rodawig, S., Jones, C., Eitel, A., Hom, P., Silliman, C.C., (2020). Succinate Activation of SUCNR1 Predisposes Severely Injured Patients to Neutrophil-Mediated ARDS. *Ann Surg*, **Publish Ahead of Print**

[29]. Subczynski, W.K., Pasenkiewicz-Gierula, M., Widomska, J., Mainali, L., Raguz, M., (2017). High Cholesterol/Low Cholesterol: Effects in Biological Membranes: A Review. *Cell Biochem Biophys.*, **75** (3–4), 369–385.

[30]. Pottecher, J., Meyer, A., Wenceslau, C.F., Timmermans, K., Hauser, C.J., Land, W.G., (2019). Editorial: Trauma-Induced, DAMP-Mediated Remote Organ Injury, and Immunosuppression in the Acutely Ill Patient. *Front Immunol.*, **10**, 1971.

[31]. Tavintharan, S., Ong, C.N., Jeyaseelan, K., Sivakumar, M., Lim, S.C., Sum, C.F., (2007). Reduced mitochondrial coenzyme Q10 levels in HepG2 cells treated with high-dose simvastatin: a possible role in statin-induced hepatotoxicity? *Toxicol Appl Pharmacol.*, **223** (2), 173–179.

[32]. Ayala, A,. Muñoz, MF,. Argüelles, S,. (2014). Lipid peroxidation: production, metabolism, and signaling mechanisms of malondialdehyde and 4-hydroxy-2-nonenal. Oxid Med Cell Longev. 2014, 360438.

[33]. Tricarico, P.M., Crovella, S., Celsi, F., (2015). Mevalonate Pathway Blockade, Mitochondrial Dysfunction and Autophagy: A Possible Link. *Int J Mol Sci.*, **16** (7), 16067–16084.

[34]. Istvan, E.S., Deisenhofer, J., (2001). Structural mechanism for statin inhibition of HMG-CoA reductase. *Science.*, **292** (5519), 1160–1164.

[35]. Miettinen, T.P., Björklund, M., (2015). Mevalonate Pathway Regulates Cell Size Homeostasis and Proteostasis through Autophagy. *Cell Rep.*, **13** (11), 2610–2620.

[36]. Moon, S.-H., Huang, C.-H., Houlihan, S.L., Regunath, K., Freed-Pastor, W.A., Morris, J.P., Tschaharganeh, D.F., Kastenhuber, E.R., Barsotti, A.M., Culp-Hill, R., Xue, W., Ho, Y.-J., Baslan, T., Li, X., Mayle, A., de Stanchina, E., Zender, L., Tong, D.R., D'Alessandro, A., Lowe, S.W., Prives, C., (2019). p53 Represses the Mevalonate Pathway to Mediate Tumor Suppression. *Cell.*, **176** (3), 564–580.e19.

[37]. Wang, B., Wu, L., Chen, J., Dong, L., Chen, C., Wen, Z., Hu, J., Fleming, I., Wang, D.W., (2021). Metabolism pathways of arachidonic acids: mechanisms and potential therapeutic targets. *Signal Transduction and Targeted Therapy.*, **6** (1), 94.

[38]. Hanna, V.S., Hafez, E.A.A., (2018). Synopsis of arachidonic acid metabolism: A review. *J Adv Res.*, **11**, 23–32.

[39]. Harizi, H., Corcuff, J.B., Gualde, N., (2008). Arachidonic-acid-derived eicosanoids: roles in biology and immunopathology. *Trends Mol Med.*, **14** (10), 461–469.

[40]. Chiang, N., Arita, M., Serhan, C.N., (2005). Anti-inflammatory circuitry: lipoxin, aspirin-triggered lipoxins and their receptor ALX. *Prostaglandins Leukot Essent Fatty Acids.*, **73** (3–4), 163–177.

[41]. Serhan, C.N., Clish, C.B., Brannon, J., Colgan, S.P., Chiang, N., Gronert, K., (2000). Novel functional sets of lipid-derived mediators with antiinflammatory actions generated from omega-3 fatty acids via cyclooxygenase 2-nonsteroidal antiinflammatory drugs and transcellular processing. *J Exp Med.*, **192** (8), 1197–1204.

[42]. Grann, M,. Comerma-Steffensen, S,. Arcanjo, DD,. Simonsen, U,. (2016). Mechanisms Involved in Thromboxane A_2-induced Vasoconstriction of Rat Intracavernous Small Penile Arteries. Basic Clin Pharmacol Toxicol. Oct;119 Suppl 3:86-95.

[43]. Haeggström, J.Z., Funk, C.D., (2011). Lipoxygenase and leukotriene pathways: biochemistry, biology, and roles in disease. *Chem Rev.*, **111** (10), 5866–5898.

[44]. Offermanns, S., (2006). Activation of platelet function through G protein-coupled receptors. *Circ Res.*, **99** (12), 1293–1304.

[45]. Lim, P., Sadre-Bazzaz, K., Shurter, J., Sarasin, A., Termini, J., (2003). DNA damage and mutations induced by arachidonic acid peroxidation. *Biochemistry.*, **42** (51), 15036–15044.

[46]. Demetz, E., Schroll, A., Auer, K., Heim, C., Patsch, J.R., Eller, P., et al., (2014). The arachidonic acid metabolome serves as a conserved regulator of cholesterol metabolism. *Cell Metab.*, **20** (5), 787–798.

[47]. Reitsma, S., Slaaf, D.W., Vink, H., van Zandvoort, M.A., oude Egbrink, MG, (2007). The endothelial glycocalyx: composition, functions, and visualization. *Pflugers Arch.*, **454** (3), 345–359.

[48]. Caterson, B., Melrose, J., (2018). Keratan sulfate, a complex glycosaminoglycan with unique functional capability. *Glycobiology.*, **28** (4), 182–206.

[49]. Toborek, M., Lee, Y.W., Garrido, R., Kaiser, S., Hennig, B., (2002). Unsaturated fatty acids selectively induce an inflammatory environment in human endothelial cells. *Am J Clin Nutr.*, **75** (1), 119–125.

[50]. Hennig, B., Watkins, B.A., (1989). Linoleic acid and linolenic acid: effect on permeability properties of cultured endothelial cell monolayers. *Am J Clin Nutr.*, **49** (2), 301–305.

[51]. Li, G., Wang, X., Yang, H., Zhang, P., Wu, F., Li, Y., Zhou, Y., Zhang, X., Ma, H., Zhang, W., Li, J., (2020). α-Linolenic acid but not linolenic acid protects against hypertension: critical role of SIRT3 and autophagic flux. *Cell Death Dis.*, **11** (2), 83.

[52]. Nemkov, T., Hansen, K.C., D'Alessandro, A., (2017). A three-minute method for high-throughput quantitative metabolomics and quantitative tracing experiments of central carbon and nitrogen pathways. *Rapid Commun Mass Spectrom.*, **31** (8), 663–673.

[53]. Catalin, E,. Doneanu, WC,. Mazzeo, RJ,. (2011). UPLC/MS Monitoring of Water-Soluble Vitamin Bs in Cell Culture Media in Minutes, Waters Application note 720004042en.

[54]. Johnsen, L.G., Skou, P.B., Khakimov, B., Bro, R., (2017). Gas chromatography – Mass spectrometry data processing made easy. *J Chromatogr A.*, **1503**, 57–64.

[55]. Volkova, S., Matos, M.R.A., Mattanovich, M., Marín, de Mas, I, (2020). Metabolic Modelling as a Framework for Metabolomics Data Integration and Analysis. *Metabolites.*, **10** (8), 303.

[56]. Heirendt, LSA,. Pfau, T,. Mendoza, SN,. Richelle, A,. Heinken,. A, Haraldsdóttir, HS,. Wachowiak, J,. Keating, SM,. Vlasov, V,. Magnusdóttir, S,. Ng, CY,. Preciat, G,. Žagare, A,. Chan, SHJ,. Aurich, MK,. Clancy, CM,. Modamio, J,. Sauls, JT,. Noronha, A,. Bordbar, A,. Cousins, B,. El Assal, DC,. Valcarcel, LV,. Apaolaza,I,. Ghaderi, S,. Ahookhosh, M,. Guebila, MB,. Kostromins, A,. Sompairac, N,. Le, HM,. Ding Ma, Sun, Y,. Wang, L,. Yurkovich, JT,. Oliveira, MAP,. Vuong, PT,. El Assal, LP,. Kuperstein, I,. Zinovyev, A,. Scott Hinton, H,. Bryant, WA,. Aragón Artacho, FJ,. Planes, FJ,. Egils Stalidzans, E,. shown) eaaan. Creation and analysis of biochemical constraint-based models: the COBRA Toolbox v3.0. https://arxivorg/abs/171004038. (Submitted on 11 Oct 2017 (v1), last revised 23 Feb 2018 (this version, v2)).

[57]. Airola, A., Pahikkala, T., Waegeman, W., De Baets, B., Salakoski, T., (2011). An experimental comparison of cross-validation techniques for estimating the area under the ROC curve. *Computational Statistics & Data Analysis.*, **55** (4), 1828–1844.

[58]. Orth, J.D., Thiele, I., Palsson, B.Ø., (2010). What is flux balance analysis? *Nature Biotechnology.*, **28** (3), 245–248.

[59]. Schonlau, M., (2004). Visualizing Hierarchical and Non-Hierarchical Cluster Analyses with Clustergrams. *Computational Statistics*, **19** (1), 95–111.